LETTERS | FOCUS
PUBLISHED ONLINE: 24 OCTOBER 2010 | DOI: 10.1038/NGEO992
nature geoscience

Transpressional rupture of an unmapped fault during the 2010 Haiti earthquake

Eric Calais[1]*, Andrew Freed[1], Glen Mattioli[2,3], Falk Amelung[4], Sigurjón Jónsson[5], Pamela Jansma[3], Sang-Hoon Hong[4], Timothy Dixon[4], Claude Prépetit[6] and Roberte Momplaisir[7]

On 12 January 2010, a M_w 7.0 earthquake struck the Port-au-Prince region of Haiti. The disaster killed more than 200,000 people and caused an estimated $8 billion in damages, about 100% of the country's gross domestic product[1]. The earthquake was initially thought to have ruptured the Enriquillo–Plantain Garden fault of the southern peninsula of Haiti, which is one of two main strike-slip faults inferred to accommodate the 2 cm yr^{-1} relative motion between the Caribbean and North American plates[2,3]. Here we use global positioning system and radar interferometry measurements of ground motion to show that the earthquake involved a combination of horizontal and contractional slip, causing transpressional motion. This result is consistent with the long-term pattern of strain accumulation in Hispaniola. The unexpected contractional deformation caused by the earthquake and by the pattern of strain accumulation indicates present activity on faults other than the Enriquillo–Plantain Garden fault. We show that the earthquake instead ruptured an unmapped north-dipping fault, called the Léogâne fault. The Léogâne fault lies subparallel to—but is different from—the Enriquillo–Plantain Garden fault. We suggest that the 2010 earthquake may have activated the southernmost front of the Haitian fold-and-thrust belt[4] as it abuts against the Enriquillo–Plantain Garden fault. As the Enriquillo–Plantain Garden fault did not release any significant accumulated elastic strain, it remains a significant seismic threat for Haiti and for Port-au-Prince in particular.

The M_w 7.0 Haiti earthquake of 12 January 2010 is the largest event to strike the southern part of Hispaniola since the 15 September 1751, 21 November 1751 and 3 June 1770 events, which also severely affected Port-au-Prince. Although the location of these historical events is poorly constrained, they are thought to have ruptured the Muertos–Enriquillo–Plantain Garden fault system[5] (Fig. 1b). They were followed on 7 May 1842 by a M_w 8.0 event farther north, inferred to occur on the offshore section of the Septentrional fault along the northern coast of Haiti, then by a sequence of M_w 7.5–8.1 events between 1946 and 1953 on the subduction fault to the northeast of the Dominican Republic (Fig. 1b).

These large earthquakes highlight the three main fault systems that accommodate the Caribbean–North America relative plate motion in the northeastern Caribbean (Fig. 1a), at the transition between frontal subduction of the North American plate beneath the Caribbean plate in the Lesser Antilles and roughly east–west strike-slip motion along the Cayman trough[6–9]. Global positioning system (GPS) studies show that the interior of the Caribbean plate moves east-northeastwards (N70 E) at a rate of 18–20 mm yr^{-1} relative to the North American plate[3,10], implying oblique convergence between Hispaniola–Puerto Rico and the oceanic lithosphere of the North American plate[11,12]. This oblique convergence is partitioned in Hispaniola between plate-boundary-parallel motion on the Septentrional and southern peninsula fault zones in the overriding plate, and plate-boundary-normal (thrust) motion at the plate interface along the north Hispaniola fault zone[13,14] (Fig. 2b). In addition, active oblique thrusting has been mapped along the southern edge of the Chaine des Matheux and its continuation in the Dominican Republic as the Sierra de Neiba (Haiti fold-and-thrust belt[4], Fig. 2b), which connect farther east, offshore, with the active Muertos trough.

GPS surveys in the Dominican Republic since 1986 (refs 3, 14) and preliminary results in Haiti since 2003 (ref. 15) may be modelled with slip rates of 9 ± 2 mm yr^{-1} on the Septentrional fault, consistent with palaeoseismic data[16], and 7 ± 2 mm yr^{-1} on the southern peninsula fault zone. From 2006 to 2009, we acquired new observation epochs at 35 GPS sites in Haiti and completed an additional survey of the Dominican Republic GPS network (see the Methods section), providing the first comprehensive velocity field for Hispaniola (Fig. 2). In a North America-fixed frame, east–west left-lateral shear and a north–south gradient in velocities are apparent (Fig. 2a), reflecting elastic strain accumulation across the plate boundary. In a Caribbean-fixed frame, an additional component of plate-boundary-normal contraction becomes apparent (Fig. 2b). This also appears on a velocity cross-section through Haiti (Fig. 2c), with about 4 mm yr^{-1} of shortening, mostly accommodated across the southern half of the island.

We model these interseismic velocities as the contribution of block rotations and elastic strain accumulation on locked, seismogenic, faults[17] (see the Methods section). The resulting kinematic model (Fig. 1b) shows slip rates of 2 ± 1 to 6 ± 1 mm yr^{-1} on the north Hispaniola reverse fault, 12 ± 2 mm yr^{-1} on the Septentrional fault zone and 5 to 6 ± 2 mm yr^{-1} on the southern peninsula fault zone. The present spatial resolution of our GPS network is not sufficient to identify smaller subfaults within these three faults zones, and therefore they are each modelled as a single strand. Model estimates on the southern peninsula fault zone imply transpression, combining left-lateral strike-slip (5 ± 1 mm yr^{-1}) and reverse slip (2 ± 1 mm yr^{-1}). If we assume that the last major events in southern Hispaniola in 1751 and 1770, about 250 years ago, occurred within that fault zone, and that elastic strain has been accumulating at a constant rate of 6 mm yr^{-1}, a total slip deficit of 1.5 m is implied. No major earthquake has been reported in southern Haiti since then, although smaller magnitude events, which are less well located, occurred in 1784, 1860, 1864 and 1953 (Fig. 2b). If entirely released in a single event, this slip deficit would

[1]Department of Earth and Atmospheric Sciences, Purdue University, Indiana 47906, USA, [2]University of Arkansas, Department of Geosciences, Fayetteville, Arkansas 72701, USA, [3]University of Texas at Arlington, Arlington, Texas 76010, USA, [4]Rosenstiel School of Marine and Atmospheric Sciences, University of Miami, Miami, Florida 33149, USA, [5]King Abdullah University of Science and Technology (KAUST), Thuwal, Saudi Arabia, [6]Bureau des Mines et de l'Energie, Port-au-Prince, Haiti, [7]Université d'Etat d'Haiti, Faculté des Sciences, Port-au-Prince, Haiti. *e-mail: ecalais@purdue.edu.

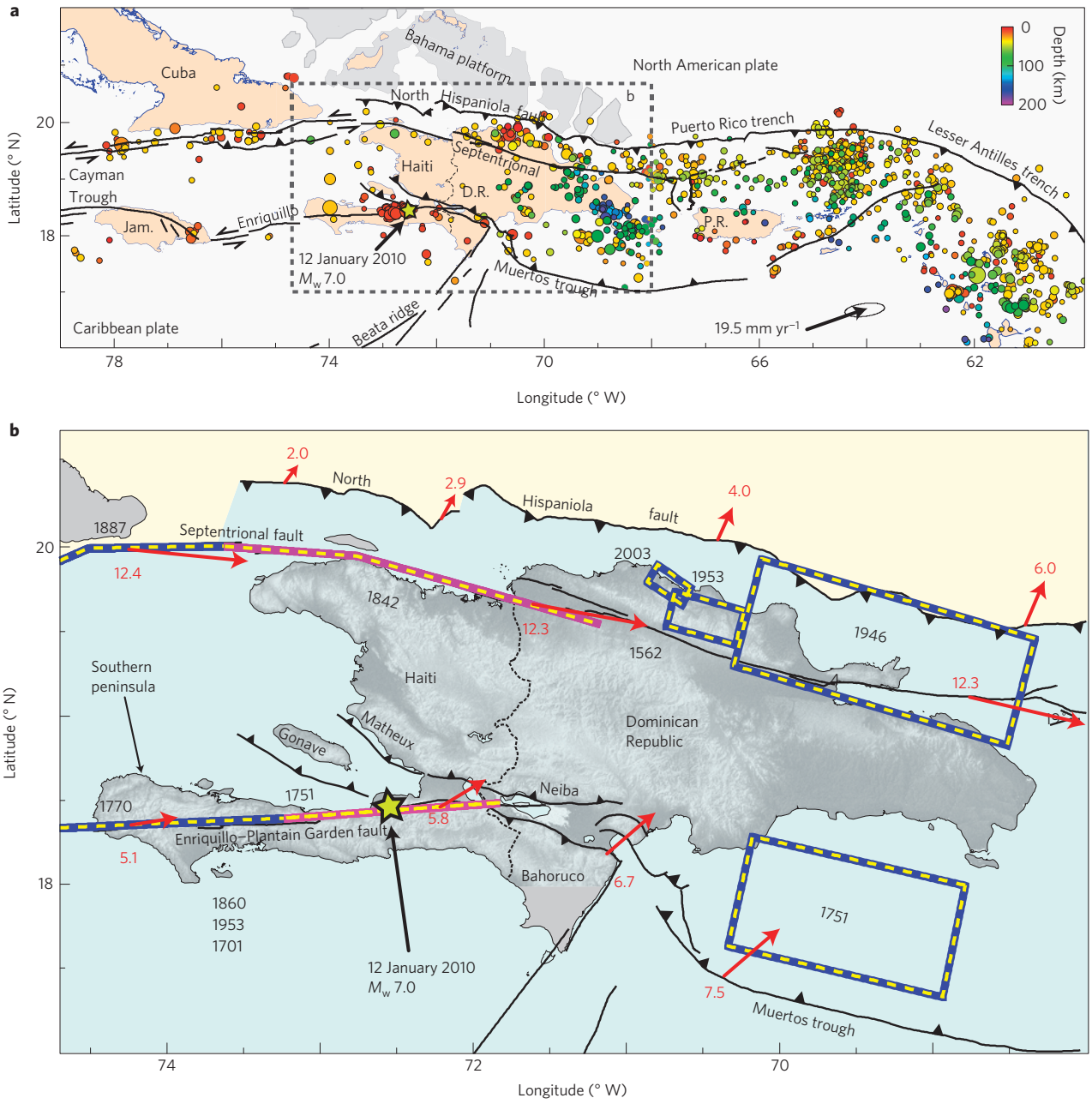

Figure 1 | Tectonic setting of the northeastern Caribbean and Hispaniola. a, Major active plate-boundary faults (black lines), instrumental seismicity (National Earthquake Information Center database, 1974–present) and Caribbean–North America relative motion[10] (arrow). P.R. = Puerto Rico; D.R. = Dominican Republic. **b**, Summary of the present-day tectonic setting of Hispaniola. Estimated historical rupture areas are derived from archives[5]. 1860, 1953 and 1701 are the dates of smaller magnitude, poorly located events. Vertical strike-slip events are shown as lines; dip-slip events are shown as projected surface areas. The red arrows show geodetically inferred long-term slip rates (labelled in mm yr^{-1}) of active faults in the region from the block model discussed here (the arrows show motion of the southern with respect to the northern block).

scale to a M_w 7.1 event[18], consistent with previous estimates[15] and with the moment magnitude of the 12 January event.

We resurveyed the Haiti GPS network between 31 January and 15 February 2010. Resulting coseismic displacements reach up to 0.7 m and 0.8 m at sites DFRT and LEOG, closest to the earthquake epicentre (Fig. 3a). Measurable coseismic displacements are observed up to ~150 km from the epicentre. The spatial distribution of horizontal coseismic displacements shows a pattern that combines left-lateral strike-slip and a significant amount of fault-perpendicular shortening in a pattern similar to the interseismic strain accumulation (Fig. 2). This is well illustrated by the baseline between sites DFRT and TROU, with 0.9 m of shortening in a N166 E direction, quasi-perpendicular to the N85 E general direction of the Enriquillo–Plantain Garden fault in that area (Fig. 3a).

Coseismic displacements are also well recorded by synthetic aperture radar interferometry. We used Advanced Land Observing Satellite/Phased Array type L-band Synthetic Aperture Radar (ALOS/PALSAR) data to compute three interferograms spanning 12 January 2010 (see the Methods section). We find significant range change over a ~50-km-wide region from Greissier in the east to Petit Goâve in the west (Fig. 4a). Line-of-sight

NATURE GEOSCIENCE DOI:10.1038/NGEO992

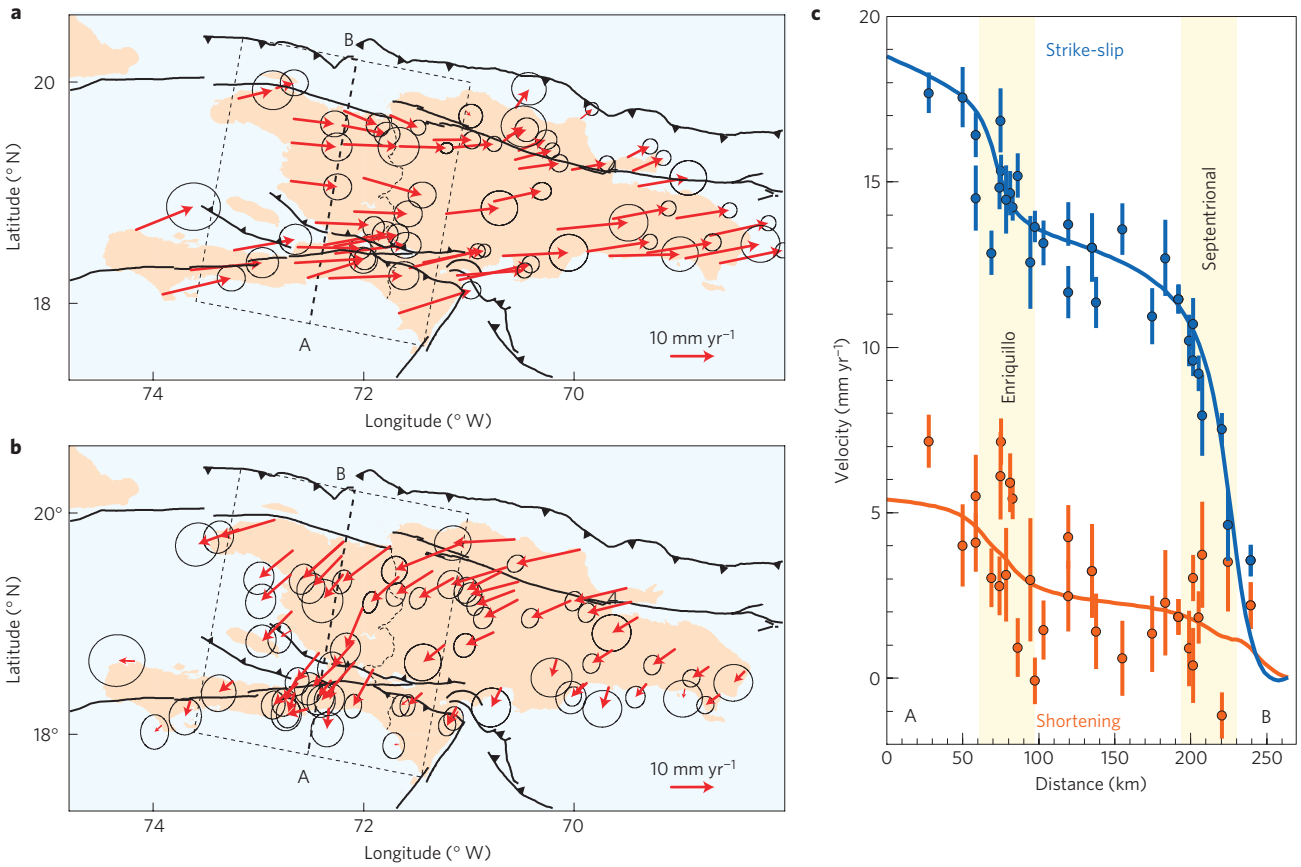

Figure 2 | Interseismic GPS velocities. The GPS velocity field is determined from GPS campaigns before the 12 January 2010 earthquake. The ellipses and error bars are 95% confidence. **a**, Velocities with respect to the North American plate. **b**, Velocities with respect to the Caribbean plate. **c**, Velocity profile perpendicular to the plate boundary (coloured circles and one-sigma error bars) and best-fit elastic block model (solid lines). Blue = profile-perpendicular ('strike-slip') velocity components; orange = profile-parallel ('shortening') velocity components. The profile trace and width are indicated by dashed lines in **a** and **b**.

displacements up to 0.9 m for the ascending track and 0.75 m for the descending one coincide with the Léogâne alluvial fan north of the mapped Enriquillo–Plantain Garden fault. Decreasing range in both ascending and descending interferograms indicates a significant amount of vertical motion (uplift), and the larger range change in the ascending interferograms indicates westward ground motion. These results are consistent with observations of coastal uplift (up to 0.6 m) from raised coral reefs along the coast from Petit Goâve to the north of Léogâne[19].

To infer the geometry of the earthquake rupture and estimate the associated coseismic slip distribution, we modelled surface deformation as the result of fault dislocations in an elastic half-space in a two-step process (see the Methods section). Given the limited information on active faults in the epicentral area, we modelled the simplest possible geometry of a single and planar fault rupture. A full description of the event may require more complex geometries. The solution to a planar, uniform slip, rupture requires that the fault dips to the north at an angle of ~60°, with its upper edge at ~5 km depth and a surface area of 32.5 × 10.5 km (Fig. 4a). This upper edge roughly coincides with the surface trace of the Enriquillo–Plantain Garden fault but is located below the topographic surface, so that the intersection of the model fault with the surface is about 2.5 km south of the Enriquillo–Plantain Garden fault trace. We find 2.6 m and 1.8 m of strike-slip and reverse dip-slip displacement, respectively, corresponding to a M_w 7.0 event (assuming a rigidity of 30 GPa). Best-fit fault strike is N78 E, slightly more north-directed than the Enriquillo–Plantain Garden fault (N85 E). This rupture geometry is generally consistent with aftershock locations from near-field seismic stations[20], which cluster to the north of the Enriquillo–Plantain Garden fault trace (Fig. 4a). The discrepancies in geometry between the mapped Enriquillo–Plantain Garden fault and the best-fit rupture model suggest that part or all of the earthquake slip occurred on a fault other than the Enriquillo–Plantain Garden fault.

In a second step we fix the fault geometry to the best-fit uniform slip solution described above and use the GPS and interferometric synthetic aperture radar (InSAR) data to estimate variable slip distribution on the rupture plane (Supplementary Fig. S1). Our preferred solution (Fig. 4b) shows up to 5.5 m of slip with a distribution in two main lobes, from depths of about 18 to 3 km. The rupture did not reach the surface in the model, consistent with the lack of surface rupture associated with the event reported from field geological observations[21]. The total model moment release is 5.04×10^{19} N m^{-1} ($M_w = 7.1$), slightly larger than computed from teleseismic data shortly after the earthquake[22,23]. Our model implies that 62% of the moment release occurred by strike-slip motion and 38% by reverse dip-slip motion (Supplementary Fig. S2). The Haiti earthquake bears similarities with the 1989 Loma Prieta earthquake in California[24] where a well-known seismic gap on the San Andreas seemed to have produced the M_w 7.1 event, but later analysis indicated that the earthquake ruptured a dipping 70° fault, different from the San Andreas, with no associated surface rupture and a significant component of reverse slip.

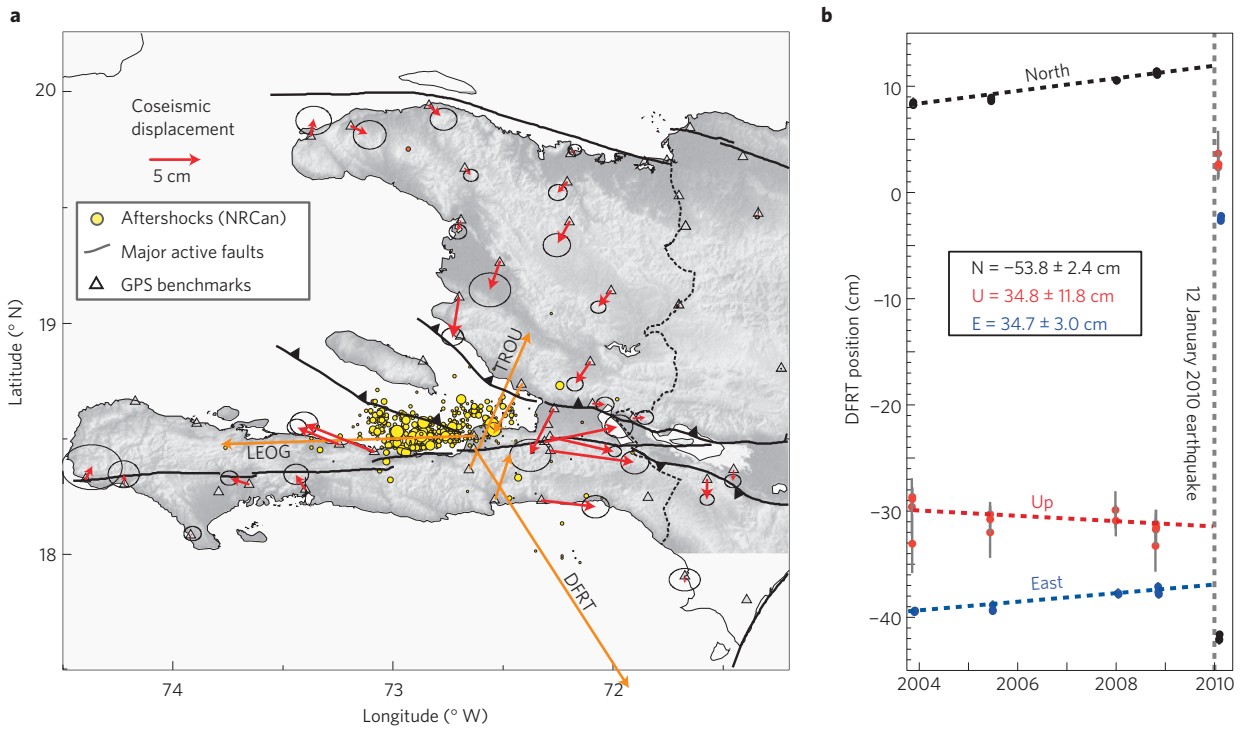

Figure 3 | Coseismic displacements from GPS measurements. a, Map of horizontal coseismic displacements. Note the significant component of shortening, similar to the interseismic velocity field (Fig. 2). The orange arrows have been shortened by 50% to fit within the map. Displacements at stations TROU and DFRT, cited in the text, are labelled. NRCan = Natural Resources Canada. **b**, Position time series at station DFRT (orange arrow labelled on **a**) showing four pre-earthquake measurement epochs and the post-earthquake epoch. Note the steady interseismic strain accumulation rate and the sudden coseismic displacement.

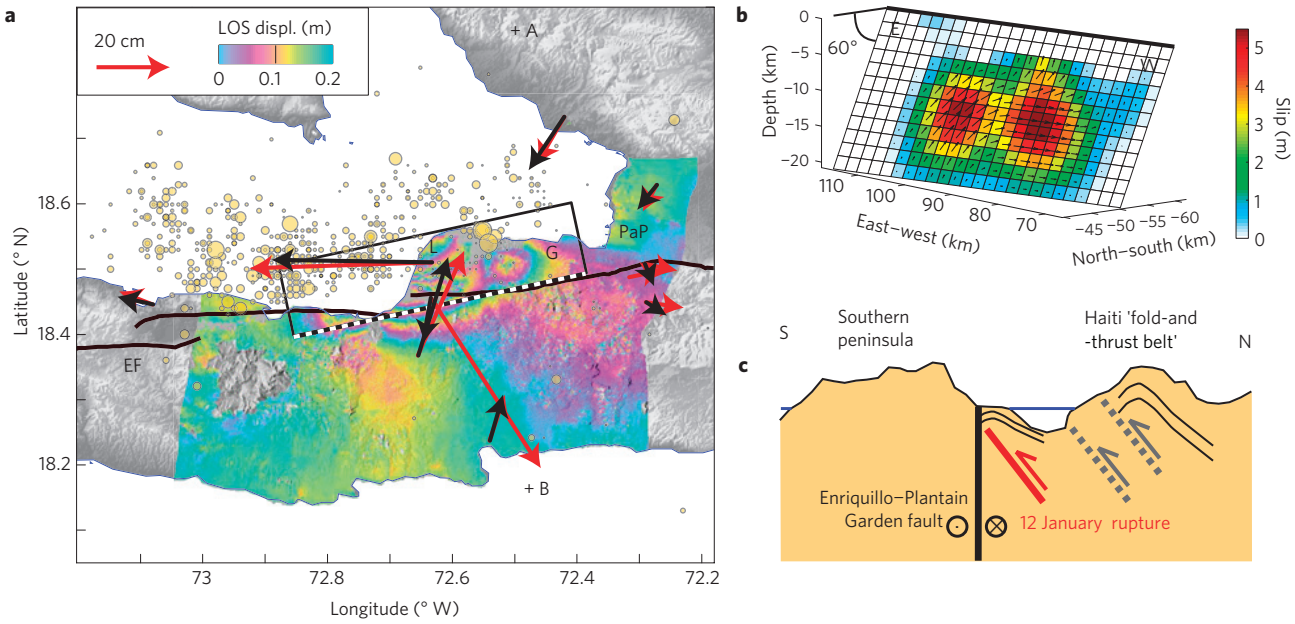

Figure 4 | Deformation observations and rupture model. a, Interferogram (descending track, constructed from images acquired on 9 March 2009 and 25 January 2010), GPS observed (black) and model (red) coseismic displacements. The yellow circles show aftershocks[20]. G = Greissier, L = Léogâne, PaP = Port-au-Prince. EF = Enriquillo–Plantain Garden fault. The black rectangle shows the surface projection of the modelled rupture; the black–white dashed line is the intersection with the surface. LOS displ. = line-of-sight displacement. **b**, Total slip distribution from a joint inversion of InSAR and GPS data, viewed from the northwest. **c**, Interpretative cross-section between points A and B indicated on **a**. The red line shows coseismic rupture.

The north-dipping geometry of the 12 January earthquake rupture and the fact that it did not reach the surface are two robust features of our source model. They are difficult to reconcile with the Enriquillo–Plantain Garden fault, as field observations along its trace near the epicentre show a vertical to high-angle (>60°) south-dipping structure with evidence of left-lateral surface

offsets during large earthquakes[21] (Fig. 4c). In addition, offset geological features and the prominent trace of the fault in the morphology both indicate that the Enriquillo–Plantain Garden fault is a long-lived feature. Repeated earthquakes similar to the 12 January event on the Enriquillo–Plantain Garden fault would have resulted in elevated topography in the hanging-wall to the north of the fault, and lower elevations to the south, opposite to the basic observation that elevated topography lies to the south of the Enriquillo–Plantain Garden fault in the epicentral area. We therefore infer that the fault responsible for the 12 January earthquake was probably not the Enriquillo–Plantain Garden fault, but rather a previously unmapped structure, possibly a blind thrust underlying the Léogâne delta, which we name the 'Léogâne fault'[19,21] (Fig. 4c). Much uncertainty remains concerning the role of this fault in the active tectonics of the region. It could be part of the southern peninsula fault zone or, alternatively, may merge at depth with the southernmost extension of the Haitian fold-and-thrust belt[4], a south-propagating system with an active frontal thrust that reaches as far south as the 1,500-m-deep basin between the southern peninsula and the Gonâve island[25].

Although the M_w 7, 12 January, Haiti earthquake did not come as a surprise given the historical seismicity and the present rate of strain accumulation in southern Haiti, several of its characteristics were unexpected. In particular, the rupture did not reach the surface and its dip angle and mechanism, well constrained by geodetic and geological data, suggest that a fault other than the Enriquillo–Plantain Garden fault has ruptured. The source mechanism, which combines left-lateral strike-slip and reverse slip on a north-dipping plane, is consistent with the secular strain accumulation pattern derived from interseismic GPS measurements. The 12 January 2010 earthquake is causing us to revise the classic thinking that present deformation in southern Haiti is accommodated by the single subvertical Enriquillo–Plantain Garden fault strike-slip fault. The significant component of contractional deformation reported here, both in the interseismic and coseismic observations, suggests that faults other than the Enriquillo–Plantain Garden fault are active, consistent with previous on-land and offshore geological mapping[4,25]. The hazard level in the greater Port-au-Prince region depends greatly on the geometry and sense of slip on these faults, both the Enriquillo–Plantain Garden fault[21] and compressional or oblique-slip structures such as the Léogâne fault. Much work remains to be done to identify and quantify potential earthquake sources in and around Hispaniola, an island where vulnerability to earthquake shaking will probably remain high in the near future.

Methods

GPS data and processing. The interseismic GPS velocity field is derived from data collected at campaign and continuous GPS sites from 1994 to 2009 in the Dominican Republic and 2003 to 2009 in Haiti. We resurveyed the Haiti GPS network between 31 January and 15 February 2010. All but one of the sites were still in place, even though most were located on buildings. We calculated coseismic displacements by projecting the site position to the date of the earthquake by fitting a straight line to the observed pre-earthquake time series for sites surveyed at least twice (30 out of 35, Fig. 3b), or using the pre-earthquake site position and the interseismic velocity as predicted by the block model (5 sites out of 35). Further details are provided in the Supplementary Information.

Block modelling. The modelling procedure divides the crust into predetermined blocks bounded by active faults locked to a certain depth and along which elastic strain accumulates. We used the elastic block modelling program 'DEFNODE' (ref. 17). DEFNODE allows for laterally variable fault coupling—in the absence of any information indicative of aseismic fault slip we imposed full coupling on all faults. DEFNODE uses GPS velocities, earthquake slip vectors and fault-specific slip rates and azimuths (where applicable) to solve for the angular velocities of the crustal blocks using a downhill simplex minimization method. Further details are provided in the Supplementary Information.

InSAR data and analysis. We used ALOS/PALSAR data from the Japan Aerospace Exploration Agency and Ministry of Economy, Trade and Industry of Japan to compute three interferograms. One interferogram from a descending orbit (satellite travelling south, track 447) was constructed from data acquired on 9 March 2009 and 25 January 2010. Two interferograms from ascending orbits (satellite travelling north) were constructed from data acquired on 8 February 2009 and 14 February 2010 (track 138), and on 28 February 2009 and 16 January 2010 (track 137). The interferograms measure ground displacement in the radar line-of-sight direction, which is about 34.5° from the vertical with a component towards the east for descending and towards the west for ascending tracks, respectively. The topographic phase was removed using a 3-arcsec (90-m)-resolution digital elevation model generated by the National Aeronautics and Space Administration Shuttle Radar Topography Mission[26], resampled to 30 m ground spacing. We used a quad-tree scheme[27] to subsample the interferograms to 232, 258 and 166 data points for descending track 447 and ascending tracks 137 and 138, respectively.

Inversion for coseismic slip. We use the coseismic GPS displacements together with three interferograms in a two-step process. We first iteratively solve for the best-fit earthquake rupture location and dip angle assuming uniform fault slip on a single planar surface. Although more complex (but poorly constrained) geometries are likely to provide a better fit to the data, we used a single fault plane because no external data (such as surface rupture or precisely relocated aftershocks) allow us to independently identify the actual rupture trace and segmentation. We solve this nonlinear inverse problem using a Monte Carlo approach that fully explores the model space, followed by a gradient method[28]. We then fix the fault geometry to the previously obtained solution and discretize the fault plane with rectangular patches of dimensions $\sim 2 \times 2$ km. We use the same data set to solve for spatially variable slip along the fault plane (further details in the Supplementary Information).

Received 28 June 2010; accepted 27 September 2010; published online 24 October 2010

References

1. Haiti Earthquake Post Disaster Needs Assessment: Assessment of damage, losses, general and sectoral needs. http://siteresources.worldbank.org/INTLAC/Resources/PDNA_Haiti-2010_Working_Document_EN.pdf (2010).
2. Mann, P., Taylor, F, Edwards, R. & Ku, T. Actively evolving microplate formation by oblique collision and sideways motion along strike-slip faults: An example from the northeastern Caribbean plate margin. *Tectonophysics* **246,** 1–69 (1995).
3. Dixon, T *et al.* Relative motion between the Caribbean and North American plates and related boundary zone deformation. *J. Geophys. Res.* **103,** 15157–15182 (1998).
4. Pubellier, M., Mauffret, A., Leroy, S., Vila, J. & Amilcar, H. Plate boundary readjustment in oblique convergence: Example of the Neogene of Hispaniola, Greater Antilles. *Tectonics* **19,** 630–648 (2000).
5. McCann, W. R. in *Estimating the Threat of Tsunamogenic Earthquakes and Earthquake-Induced Landslide Tsunami in the Caribbean* (eds Aurelio, M. & Philip, L.) 43–65 (World Scientific Publishing, 2006).
6. Mann, P., Burke, K. & Matumoto, T. Neotectonics of Hispaniola: Plate motion, sedimentation, and seismicity at a restraining bend. *Earth Planet. Sci. Lett.* **70,** 311–324 (1984).
7. Calais, E. & de Lépinay, B. From transtension to transpression along the northern Caribbean plate boundary off Cuba: Implications for the recent motion of the Caribbean plate. *Tectonophysics* **186,** 329–350 (1991).
8. Calais, E., Béthoux, N. & de Lépinay, B. From transcurrent faulting to frontal subduction: A seismotectonic study of the northern Caribbean plate boundary from Cuba to Puerto Rico. *Tectonics* **11,** 114–123 (1992).
9. Calais, E., Perrot, J. & de Lépinay, B. Strike-slip tectonics and seismicity along the northern Caribbean plate boundary from Cuba to Hispaniola. *Geol. Soc. Am. Spec. Pap.* **326,** 125–169 (1998).
10. DeMets, C. *et al.* GPS geodetic constraints on Caribbean-North America plate motion. *Geophys. Res. Lett.* **27,** 437–441 (2000).
11. Calais, E. & de Lépinay, B. Semiquantitative modeling of strain and kinematics along the Caribbean/North America strike-slip plate boundary zone. *J. Geophys. Res.* **98,** 8293–8308 (1993).
12. Mann, P. *et al.* Oblique collision in the northeastern Caribbean from GPS measurements and geological observations. *Tectonics* **21,** 1057 (2002).
13. Dolan, J., Mullins, H. & Wald, D. Active tectonics of the north-central Caribbean: Oblique collision, strain partitioning, and opposing subducted slabs. *Geol. Soc. Am. Spec. Pap.* **326,** 1–62 (1998).
14. Calais, E. *et al.* Strain partitioning and fault slip rates in the northeastern Caribbean from GPS measurements. *Geophys. Res. Lett.* **29,** 1856 (2002).
15. Manaker, D. M. *et al.* Interseismic plate coupling and strain partitioning in the northeastern Caribbean. *Geophys. J. Int.* **174,** 889–903 (2008).
16. Prentice, C., Mann, P., Peña, L. & Burr, G. Slip rate and earthquake recurrence along the central septentrional fault, north American–Caribbean plate boundary, Dominican Republic. *J. Geophys. Res.* **108,** 2149 (2003).
17. McCaffrey, R. in *Plate Boundary Zones* (eds Stein, S. & Freymueller, J.) 101–122 (AGU Geodynamics Series, Vol. 30, 2002).

18. Wells, D. & Coppersmith, K. New empirical relationships among magnitude, rupture length, rupture width, rupture area, and surface displacement. *Bull. Seismol. Soc. Am.* **4,** 974–1002 (1994).
19. Hayes, G. P. *et al.* Complex rupture during the 12 January 2010 Haiti Earthquake. *Nature Geosci.* **3,** 800–805 (2010).
20. http://earthquakescanada.nrcan.gc.ca/haiti/.
21. Prentice, C. *et al.* Seismic hazard of the Enriquillo-Plantain Garden fault in Haiti inferred from palaeoseismology. *Nature Geosci.* **3,** 789–793 (2010).
22. http://earthquake.usgs.gov/earthquakes/recenteqsww/Quakes/us2010rja6.php.
23. http://www.tectonics.caltech.edu/slip_history/2010_haiti/.
24. Hanks, T. & Krawinkler, H. The 1989 Loma Prieta earthquake and its effects: Introduction to the special issue. *Bull. Seismol. Soc. Am.* **81,** 1415–1423 (1991).
25. BienAimé-Momplaisir, R. *Contribution to the Geologic Study of the Eastern Part of the Massif of La Hotte (Presqu'Ile du Sud d'Haiti). Structural Synthesis of the Margins of the Peninsula from Seismic Data.* Doctoral thesis, Pierre et Marie Curie University, Paris, France (1986).
26. Farr, T. G. & Kobrick, M. Shuttle Radar Topography Mission produces a wealth of data. *Eos Trans. AGU* **81,** 583–585 (2000).
27. Jonsson, S., Zebker, H. & Segall, P. Fault slip distribution of the M_w 7.2 Hector Mine earthquake estimated from satellite radar and GPS measurements. *Bull. Seismol. Soc. Am.* **92,** 1377–1389 (2002).
28. Cervelli, P., Murray, M. & Segall, P. Estimating source parameters from deformation data, with an application to the March 1997 earthquake swarm off the Izu Peninsula, Japan. *J. Geophys. Res.* **106,** 11217–11237 (2001).

Acknowledgements

The results presented here owe to many collaborators, contributors and friends in Haiti, in particular the National System for Disaster Risk Reduction (A. Nazaire) and the Civil Protection Agency (A. Jean-Baptiste), the Bureau of Mines and Energy (D. Anglade) and the National Center for Geospatial Information (G. Porcena and B. Piard). M. Jeannite and F. S. Preux from the Bureau of Mines and Energy carried out the bulk of the GPS fieldwork in Haiti. We thank D. Anglade (General Director) and S. L. Mildor (Director for Geology) from the Bureau of Mines and Energy for their constant support. The post-earthquake GPS survey benefited from field support from D. Sarah Stamps and E. Chaussard. UNAVCO provided outstanding support to the field operations in Haiti. A. Holsteinson (Holasa Inc.) carried out the 2009 and 2010 GPS measurements in the Dominican Republic. The ALOS data were provided by GEO's Geohazard Supersites and are copyrighted by the Ministry of Economy, Trade and Industry of Japan and Japan Aerospace Exploration Agency. This research was supported by grants from the National Science Foundation (grants no 0409487 and RAPID no 1024990 to E.C., no 0408978 to G.M./P.J.) and the National Disaster Risk Management System Development Program-UNDP Haiti.

Author contributions

E.C. conceived the study and prepared the main manuscript, with contributions from all co-authors. All co-authors contributed to the interpretation. In addition, R.M., A.F. and G.M. contributed to the G.P.S. field work, F.A., S.J. and S-H.H. contributed the InSAR analysis, S.J. contributed the coseismic slip estimation and error analysis and P.J., T.D., R.M. and C.P. provided background context for the study. All authors discussed the results and implications and commented on the manuscript at all stages.

Additional information

The authors declare no competing financial interests. Supplementary information accompanies this paper on www.nature.com/naturegeoscience. Reprints and permissions information is available online at http://npg.nature.com/reprintsandpermissions. Correspondence and requests for materials should be addressed to E.C.